Int. J. Electrochem. Sci., 17 **(2022)** Article Number: 220763, doi: 10.20964/2022.07.65

International Journal of
ELECTROCHEMICAL
SCIENCE
www.electrochemsci.org

Short Communication

A NH_3 Gas Sensor Based on Flexible Copper(II) isonicotinate MOF /Reduced Graphene Oxide Composite Modified Interdigital Electrode

Chunping Gao, Tao Wang, Xueliang Wang[*]

School of Chemistry and Chemical Engineering, Heze University, 274015, China
[*]E-mail: yuzywxl@163.com

Received: 30 March 2022 / *Accepted:* 23 May 2022 / *Published:* 6 June 2022

The extensive application of the graphene-based composites in gas sensing was severely suffered from its poor selectivity although these materials have excellently physi-chemical properties. Herein, a flexible $Cu(INA)_2$/GO composite was synthesized in situ through a simple method. Characterization results exhibited that the intimate interfacial contact between $Cu(INA)_2$ and GO was achieved. After the GO was transformed into the reduced graphene oxide (rGO) via an electrochemical method on an interdigital electrode (IDE), the composite showed good performance for sensing NH_3 gas. The response signal intensity was linearly with the concentration of NH_3 gas in nitrogen from 50 to 500 ppm. The $Cu(INA)_2$ and rGO played synergistic effects for sensing NH_3 gas, which can provide a paradigm for the application of the Graphene-based composites in determination of the contamination gases.

Keywords: $Cu(INA)_2$/rGO composite; Reduced graphene oxide; Interdigital electrode; Gas sensing; NH_3

1. INTRODUCTION

Ammonia (NH_3) with colorless, pungent, corrosive and high toxic gas, is a by-product of the manufacturing, chemical and fossil fuel combustion [1]. Its olfactory detetion limit is about 55 ppm [2], and it is a serious threat to the atmosphere and human health [3, 4]. Exposure to ammonia at low concentrations, such as 50-100 ppm, can lead to respiratory allergies and higher exposure concentrations can cause fatal disease. Furthermore, many studies have showed that NH_3 plays a vital role in the formation of $PM_{2.5}$ (the particles with aerodynamic diameters of ＜2.5 μm in the air). In air, NH_3 can form NH_4NO_3, $(NH_4)_2SO_3$, and NH_4HSO_4 together with SO_2 and NO_X, which are important component of $PM_{2.5}$ [5, 6]. The problems together with the release of ammonia have aroused people's

increasing concern and rapid progress in the field of NH_3 sensing. Therefore, for environmental monitor and chemical control in medical, industrial and agricultural fields, it is necessary to detect the low concentrations NH_3 [7, 8].

Graphene is a famous carbon material and it has been widely applications in the field of electronics with a single-atom thick, two-dimensional sheet of sp2 bonded carbon [9]. The gas sensors based on graphene have been used for investigating NH_3, NO_2, H_2 and CO [10-12]. However, these kinds of sensors still exist some problems and shortcomings, such as poor selectivity, repeatability, stability, and only less kinds of gases can be detected, which to a large extent limited its application scope. Studies have shown that graphene can be combined with other materials to improve its electronic conductivity and stability. [13]. Therefore, in order to improve the sensing performance for gas, metal oxide, metal and organic polymer have been used to hybridize with graphene and fabricate NH_3 gas sensors [14-17].

Metal organic frameworks (MOFs) with high porosity structure and diversity of the metallic centers and organic ligands have been studied in the fields of gas storage, gas separation, and gas purification [18]. According to recent research, MOFs/graphene composites have higher stability, higher conductivity and higher selectivity than pure MOFs [18]. Even though the $Cu(INA)_2$ has been studied in NH_3 adsorption and capture a three-dimensional (3D) as a porous flexible MOF[19], the evaluation of its applicability as a sensing material for toxic gases still has not been studied. Taking into account the good performance of $Cu(INA)_2$ as ammonia adsorbents, in this research, the sensing function of the $Cu(INA)_2$/rGO composite material for different concentrations of ammonia was examined, and we reasoned that the synergistic effects of the two components in this composite material can create a mechanism for charge carrier migration.

2. MATERIALS AND METHODS

2.1 Materials and Characterization

The interdigitated electrode (IDE) was fabricated by Suzhou Nano Fabrication Facility (China). Cupric Nitrate and isonicotinic acid (HINA) were obtained from Adamas-beta Chemical Reagent Co., Ltd. Graphite powder was obtained from Nanjing Xianfeng Nano Co., Ltd. (China). Ethanol was purchased from Tianjing Damao Chemical Co., Ltd. (China). Potassium dihydrogen phosphate and Sodium hydroxide were purchased from Sinopharm Chemical Reagent Co., Ltd. Doubly distilled water (DDW) was lab-made, and all measurements were carried out at room temperature. All the chemicals used in this work, were of analytical grade.

Rigaku Mini Flex II X-ray diffractometer (XRD) measured the crystallinity and phase purity of the materials. Fourier-transform infrared (FT-IR) were carried out on a FT-IRIS50. The scanning electron microscopy (SEM) using a Hitachi on a S4800 operated at 10.0 Kv acquired morphological data. Thermogravimetric analyses (TGA) were measured on a STA449F3 thermal degradation analyzer (Germany). Electrochemical experiments were carried out on the CHI 660E (P. R. China) electrochemical workstation with the conventional three-electrode system consisted of a IDE or

modified IDE as working electrode, platinum wire as counter electrode and Ag/AgCl (saturated KCl solution) as reference electrode.

2.2 Preparation of $Cu(INA)_2$/GO nanocomposite

Commercial graphite powder was oxidized to prepare GO by Hummers' method [20]. The $Cu(INA)_2$ was synthesized by an improved method [19]. In short, 0.242 g $Cu(NO_3)_2 \cdot 3H_2O$ was dissolved in 4 mL DDW, and 0.246 g HINA was dissolved in 13 mL ethanol. Then the mixture was reacted at 80 ˚C by hydrothermal method for 24 h. The blue powder was obtained by filtration, washed with ethanol, and dried in vacuum at 80 ˚C finally. The $Cu(INA)_2$/GO composites were prepared according to a modified preparation method of $Cu(INA)_2$. Firstly, $Cu(INA)_2$ and HINA were mixed with ethanol/DDW/GO solution by sonication at 100 W for 1 h. Then, the mixture was treated hydrothermally at 80 ˚C for 24 h. Finally, the $Cu(INA)_2$/GO were obtained by washing with ethanol and drying at 80°C in vacuum. After that, the composite was grounded into a slurry using ethanol as solvent, and then the slurry was spread onto a thin-film gold IDE which had been pretreated as follows: IDEs were washed with ethanol, then DDW, and finally vacuum-dried at room temperature for 24 h. The finally modified electrode was obtained after it was dried at room temperature for 5 h.

2.3 Fabrication of the $Cu(INA)_2$/GO on an IDE

The GO in the $Cu(INA)_2$/GO composites was electrochemically reduced by immersing the $Cu(INA)_2$/GO/IDE into 0.1 M phosphate-buffered saline (PBS) (pH = 7.0), and a cyclic voltammetry was performed between -2.0 and 1.0 V, and finally it reached a steady curve. The prepared electrode was marked as $Cu(INA)_2$/rGO/IDE. The rGO/IDE was obtained by the reduction of GO/IDE in 0.1 M PBS (pH = 7.0) using the same method as above.

2.4 Sensing procedure

The IDE and the mini test vacuum chamber were showed in Figure 1. Experiments were carried out in a controlled temperature chamber at room temperature. Firstly, the samples were activated 1 hour under vacuum. Then, the gas bag was purged with pure nitrogen. Nitrogen gas was used as a carrier gas, diluting NH_3 to the desired concentration. The sensor was stored in the vacuum chamber. The gas sensing setup is connected with the electrochemical workstation

Figure 1. Interdigital electrodes (IDE)(Left) and the the mini test vacuum chamber (Right)

3. RESULTS AND DISCUSSION

3.1 XRD and Raman Study

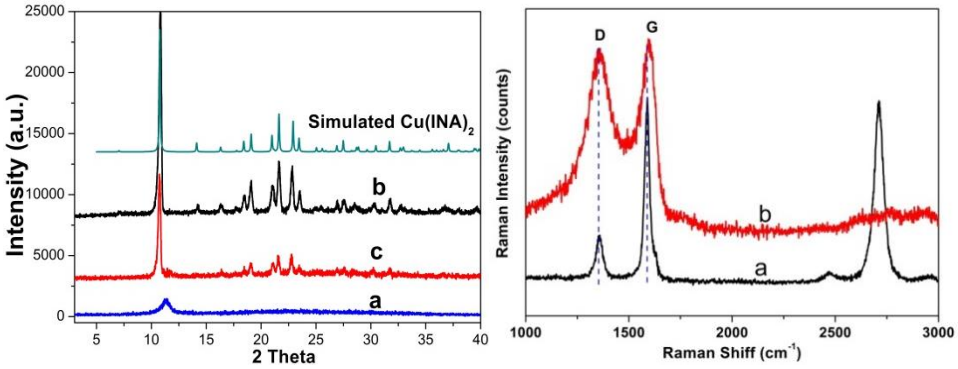

Figure 2. (Left) XRD curves of GO (a), $Cu(INA)_2$ (b) and $Cu(INA)_2$/GO (c); (Right) Raman spectra of graphene (a) and GO (b)

The XRD curves of GO (a), $Cu(INA)_2$ (b) and $Cu(INA)_2$/GO (c) were showed in Fig.2 (Left). Through comparison, it was found that all the diffraction peaks of the crystalline $Cu(INA)_2$ were remained in the composite of $Cu(INA)_2$/GO. This indicated that the crystallinity of the $Cu(INA)_2$ component was not disrupted by the interaction with GO under in-situ synthesis method. Fig.1 (Right) show Raman spectra of graphene (a) and GO (b). The Raman characteristic peaks of graphene are D peak (1350 cm^{-1}), G peak (1600 cm^{-1}) and 2D peak (~2677 cm^{-1}), which are related to the in-plane vibration of graphitic lattice and the G peak and D peak is related to defects, imperfections and edge. The peak of 1350 cm^{-1} and 1600 cm^{-1} were D peak and G peak of GO, respectively. The intensity of the G peak was lower than that of the D peak, indicating that the prepared GO was of high quality [21].

3.2 The morphologies Study

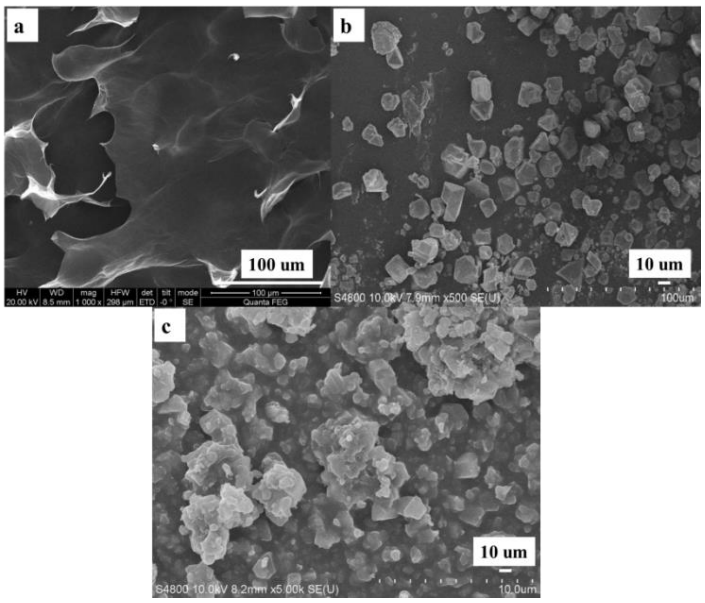

Figure 3. SEM images of GO (a), $Cu(INA)_2$ (b) and $Cu(INA)_2$/GO (c)

The SEM image of GO in Figure 3 (a) shows that graphene sheets were wrinkled with agglomerates. The SEM image of the prepared $Cu(INA)_2$ were displayed in Figure 3(b). Large quantity regular and independent analogy squares were obtained, suggesting that $Cu(INA)_2$ had high yield and good crystallinity and the octahedral shape of crystals was apparent. As the same time, the surface morphologies of $Cu(INA)_2$ composites changed obviously due to the incorporation of GO.

3.4 TGA and FTIR Study

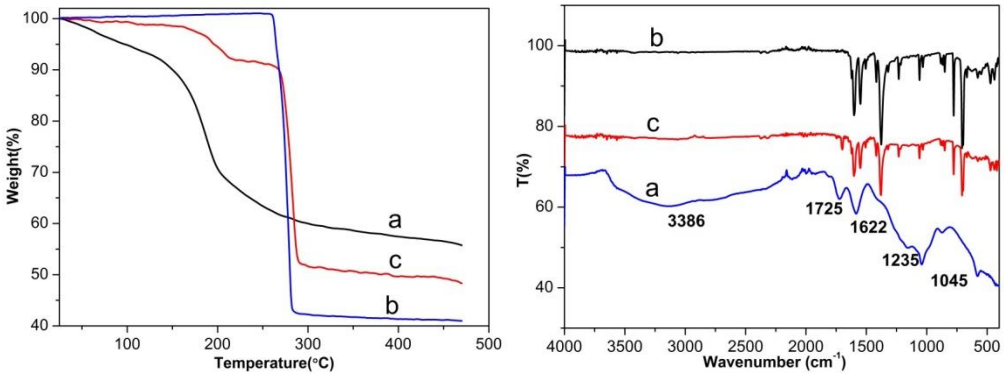

Figure 4. TGA of GO (a), $Cu(INA)_2$ (b) and $Cu(INA)_2$/GO (c) (Left); FT-IR spectra of GO (a), $Cu(INA)_2$ (b) and $Cu(INA)_2$/GO (c) (Right)

Figure 4 (Left) showed TGA of GO (a), $Cu(INA)_2$ (b) and $Cu(INA)_2$/GO (c). The thermal desorption of the water molecules physically adsorbed onto the hydrophilic GO surface led to weightlessness of GO below 150°C and the weightlessness of oxygen-containing functional groups led to the significant lose at about 200°C [22]. $Cu(INA)_2$ began to decompose at 250°C. The TGA curve

tended to be stable and the weight loss phenomenon was not obvious at above 270 °C and it showed no significant weightlessness. The first loss of weight at 150°C was due to GO adsorbed water molecules, and then the second at 250°C and this was consistent with the thermogravimetric data of GO and $Cu(INA)_2$.

The FT-IR spectra curves of GO (a), $Cu(INA)_2$ (b) and $Cu(INA)_2$/GO (c) were displayed in Fig. 4 (Right). For GO (a), the characteristic vibrations of O-H and C=O bonds appeared at 3386 cm^{-1} and 1725 cm^{-1}, respectively. The stretching vibrations peaks of C-OH and C-O-C (epoxy) appeared at 1235 cm^{-1} and 1045 cm^{-1}, respectively. The peak at 1622 cm^{-1} (skeletal vibrations),1235 cm^{-1} (C-OH) and 1045 cm^{-1} (C-O-C) were vanished. After interaction with $Cu(INA)_2$. In addition, the spectrum of $Cu(INA)_2$/GO (c) contained the characteristic peaks of $Cu(INA)_2$, suggesting that the $Cu(INA)_2$ retained its original structure after the addition of GO.

3.5 Application in Sensing Gas

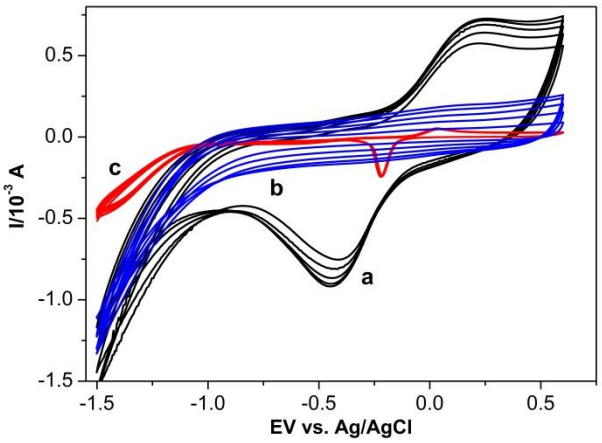

Figure 5. CVs of $Gu(INA)_2$/GO/IDE (a), $Cu(INA)_2$/IDE (b) and GO/IDE (c) in 0.1 M PBS (pH 7.0)

The electrochemical reduction is the advantage of direct, high-efficiency and eco-friendly preparation of GO reduced form [23]. In this work, the GO in the $Cu(INA)_2$/GO composites was electrochemically reduced by performing a successive cyclic voltammetry in the potential range from -2.0 to 1.0 V in the 0.1 M phosphate-buffered saline (PBS) of pH = 7.0 on a $Cu(INA)_2$/GO/IDE, and finally it reached a steady curve. The resulting electrode was named as $Cu(INA)_2$/rGO/IDE. The rGO/IDE was obtained from a GO/IDE by the same reduction procedure as above. The successive cyclic voltammetric curves for preparation of $Cu(INA)_2$/rGO/IDE (curve a) and rGO/IDE (curve c) were showed in the Figure 5. As a control, the same protocol was also performed on the $Cu(INA)_2$/IDE (curve b). It was found that the redox peaks were continually increased on the $Cu(INA)_2$/rGO/IDE or rGO/IDE with number of circle increased. However, on a the $Cu(INA)_2$/IDE, the CV curve hardly changes during the throughout scan process (Figure 5(b)). The results indicated that the GO nanosheets on the $Cu(INA)_2$/GO/IDE or GO/IDE were gradually transformed into rGO which possesses high conductivity with number of circle increased. The redox signal of GO/IDE was obviously smaller than

that of $Cu(INA)_2$/GO/IDE can be ascribed to the lower electron transfer rate on the GO/IDE[24]. This indicated that the electrochemical reduction of GO on the IDE was also affected by $Cu(INA)_2$ in the composite.

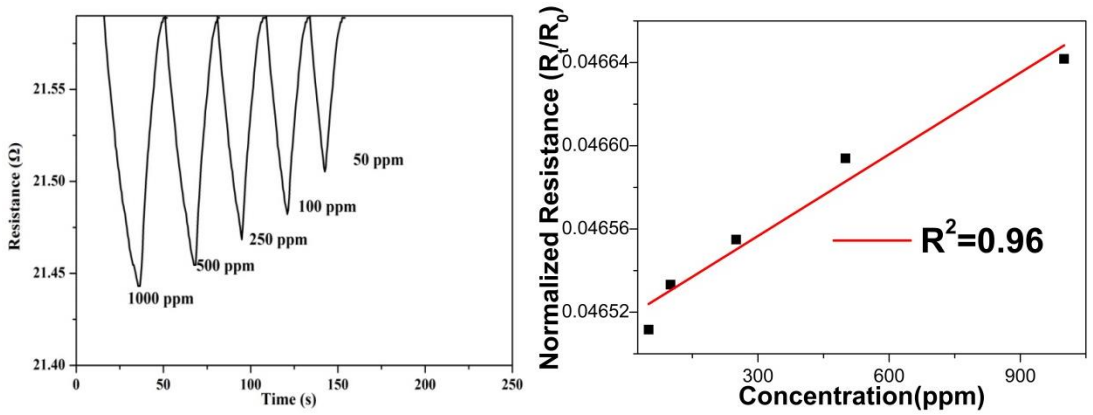

Figure 6. (Left) Detection of NH_3 in different range of concentrations for $Cu(INA)_2$/rGO/IDE; (Right) Calibration curve for the corresponding range

The sensing performance of the $Cu(INA)_2$/rGO/ID was investigated by exposed the modified electrode to different concentrations of NH_3 in nitrogen, ranging between 50 and 500 ppm. Figure 6 (Left) showed the normalized changes in the resistance. The higher the concentration of NH3 was, the stronger the signal became at a fixed exposure time. This is because more NH_3 would be physically adsorbed in the micropores via the pore filling mechanism. Because of $Cu(INA)_2$ with good adsorption performance for NH_3, the signal of $Cu(INA)_2$/rGO/ID sensor was stronger compared to other NH_3 sensors. And the further studies showed that the response destiny of NH_3 on the $Cu(INA)_2$/rGO/IDE was linearly with the concentration of NH_3 in the ppm range from 50 to 500 with R^2 = 0.96 Fig. 6 (Right). According to the gas sensing results, the $Cu(INA)_2$/rGO/IDE has outstanding sensing properties for NH_3 at room temperature. There are two aspects to explain this phenomenon. For one thing, the gas molecules are more easily diffused and adsorbed in the flexible $Cu(INA)_2$. Meanwhile, more activated sites will also be provided due to the high specific surface area of $Cu(INA)_2$ and promote the gas adsorption[19]. For another, the synergistic effects of the two components in the composite materials on the conductivity can create a mechanism for carrier mobility. The adsorption capacity of $Cu(INA)_2$ combined with good electrical conductivity of the graphene-based phase allows it to be used as a component of safety devices. By adsorbing NH_3 and measuring the air quality at the same tiome, users are prevented from being exposed to the environment..

4. CONCLUSIONS

In summary, the $Cu(INA)_2$/GO composite material was prepared in situ by a simple method and the composite was coated on an IDE to construct a gas sensor for detecting the NH_3 gas with low

concentration in N_2. This sensor combined the high selective adsorption performance of $Cu(INA)_2$ on the low concentration NH_3 with the unique electrochemical response of GO, and showed the synergistic effect for NH_3 gas sensing. This kind of sensors is a useful tool to detect contamination gases.

ACKNOWLEDGEMENT
This research is funded by Shandong Natural Science Foundation of China (grant number ZR2019BB082) and Fujian Provincial Key Laboratory of Modern Analytical Science and Separation Technology, Minnan Normal University (grant number 2020KFKT-02).

References

1. B. Timmer, W. Olthuis, A. Van Den Berg, *Sensors and Actuators B: Chemical*, 107 (2005) 666-677.
2. M. Bendahan, P. Lauque, C. Lambert-Mauriat, H. Carchano, J. L. Seguin, *Sensors and Actuators B: Chemical*, 84 (2002) 6-11.
3. M. Karami, P. Keshavarz, M. Khorram, M. Mehdipour, *Journal of hazardous materials*, 260 (2013) 576-584.
4. S.N. Behera, M. Sharma, V.P. Aneja, R. Balasubramanian, *Environmental Science and Pollution Research*, 20 (2013) 8092-8131.
5. L. Yang, A.D. Kent, X. Wang, T.L. Funk, R.S. Gates, Y. Zhang, *Journal of Hazardous Materials*, 271 (2014) 292-301.
6. J. Heo, S.T. McCoy, P.J. Adams, *Environmental Science & Technology*, 49 (2015) 5142-5150.
7. Y.S. Lee, K.D. Song, J.S. Huh, W.Y. Chung, D.D. Lee, *Sensors and Actuators B: Chemical*, 108 (2005) 292-297.
8. T. Hibbard, K. Crowley, F. Kelly, F. Ward, J. Holian, A. Watson, A.J. Killard, *Analytical chemistry*, 85 (2013) 12158-12165.
9. F. Krach, S. Hertel, D. Waldmann, J. Jobst, M. Krieger, S. Reshanov, A. Schöner, H.B. Weber, *Applied Physics Letters*, 100 (2012) 122102.
10. F. Schedin, A.K. Geim, S.V. Morozov, E. Hill, P. Blake, M. Katsnelson, K.S. Novoselov, *Nature materials*, 6 (2007) 652-655.
11. H.E. Romero, P. Joshi, A.K. Gupta, H.R. Gutierrez, M.W. Cole, S.A. Tadigadapa, P.C. Eklund, *Nanotechnology*, 20 (2009) 245501.
12. R. Arsat, M. Breedon, M. Shafiei, P. Spizziri, S. Gilje, R. Kaner, K. Kalantar-zadeh, W. Wlodarski, *Chemical Physics Letters*, 467 (2009) 344-347.
13. Y. Yang, Z. Lin, S. Gao, J. Su, Z. Lun, G. Xia, J. Chen, R. Zhang, Q. Chen, *Acs Catalysis*, 7 (2017) 469-479.
14. Z.U. Abideen, J.H. Kim, A. Mirzaei, H.W. Kim, S.S. Kim, *Sensors and Actuators B: Chemical*, 255 (2018) 1884-1896.
15. M. Zhou, Y.H. Lu, Y.Q. Cai, C. Zhang, Y.P. Feng, *Nanotechnology*, 22 (2011) 385502.
16. Z. Wu, X. Chen, S. Zhu, Z. Zhou, Y. Yao, W. Quan, B. Liu, *Sensors and Actuators B: Chemical*, 178 (2013) 485-493.
17. P. Mishra, S. Edubilli, B. Mandal, S. Gumma, *The Journal of Physical Chemistry C*, 118 (2014) 6847-6855.
18. Y. Zheng, S. Zheng, H. Xue, H. Pang, *Advanced Functional Materials*, 28 (2018) 1804950.
19. Y. Chen, L. Li, J. Li, K. Ouyang, J. Yang, *Journal of hazardous materials*, 306 (2016) 340-347.
20. W.S. Hummers Jr, R.E. Offeman, *Journal of the american chemical society*, 80 (1958) 1339-1339.
21. W. Chen, L. Yan, P.R. Bangal, *Carbon*, 48 (2010) 1146-1152.

22. T.A. Pham, B.C. Choi, K.T. Lim, Y.T. Jeong, *Applied Surface Science*, 257 (2011) 3350-3357.
23. X. Xu, D. Huang, K. Cao, M. Wang, S.M. Zakeeruddin, M. Grätzel, *Scientific reports*, 3 (2013) 1-7.
24. C. Liu, K. Wang, S. Luo, Y. Tang, L. Chen, *small*, 7 (2011) 1203-1206